Reflectance and Shape from Image Sequence of a Rotating Object

Jiping Lu & Jim Little
Laboratory for Computational Intelligence
Department of Computer Science
The University of British Columbia
Vancouver B.C., Canada V6T 1Z4
e-mail: jplu@cs.ubc.ca & little@cs.ubc.ca

Abstract

Most shape-from-shading techniques require that the reflectance function, the mapping from surface orientation to image brightness, be known or be in some particular form. In this paper we show that the reflectance function of a rotating object illuminated under a collinear light source can be estimated from the image sequence of the object and applied to surface recovery. We first calculate the 3D locations for a set of singular points from the image sequence, and extract the brightness values of these singular points from the image sequence to estimate the reflectance function. Then we use the estimated reflectance function and two images of the rotating object for surface recovery. In surface recovery, we exploit both photometric constraints and and geometric constraints on the correspondence of a surface point in the two images and use first-order Taylor series approximation to recover surface depth and orientation simultaneously. The experimental results on real image sequence show that the method is feasible and robust.

1 Introduction

Based on physical properties of the reflectance of a surface, shading in images can be used for surface recovery. A lot of work, for example, shape from shading [2, 8], photometric stereo [14, 15, 16], and photometric sampling [4], has been done in this area. In order to use shading information, the reflectance function of the surface under recovery is usually assumed to be known or computed from images. The most common assumption on surface reflectance is Lambertian reflectance [12, 8] because of its simplicity. In photometric stereo [15, 16], the reflectance function is computed from a calibration object which has the same surface reflectance function as that of the object under recovery.

However, for most real objects, the surface reflectance is not Lambertian. The Lambertian assumption is only valid in some limited cases and limited lighting and viewing conditions [13, 11, 6]. Empirical photometric stereo [15, 16] requires that the calibration object and the object under recovery have the same reflectance function and be illuminated and viewed under the same conditions. The calibration process may become difficult or impossible when we cannot find a suitable calibration object.

In our technique, we attempt to estimate the surface reflectance function directly from image sequence of a rotating object and then use the estimated reflectance function to recover the scaled surface depth and surface orientation of the object. The object is mounted on a turntable whose rotation angle can be controlled or detected. A *collinear* light source, which points in the same direction as the camera viewing direction, gives a uniform radiance over the object. The images are taken by a fixed camera while the object rotating around a vertical axis. Under the illumination of a collinear light source, the image brightness of a surface point is a function of the incident angle i, which is the angle between the illuminant direction and the surface normal. This fact makes it easy to estimate the reflectance function and apply the reflectance function for surface recovery.

The estimation of the reflectance function is based on a set of singular surface point whose incident angles are zero. The 3D coordinates of the singular points are computed from image points of the maximum brightness values and the corresponding

contour points in the image sequence. Using the 3D locations of these singular points, their brightness values in the image sequence are extracted. The correspondence between their image brightness values and their incident angles during the rotation are used for building the reflectance function.

Surface recovery is done by using two images in the image sequence. It starts from the singular points which are used to extract the surface reflectance function. Applying first-order Taylor series approximation, the 3D coordinates of the neighbor points of a singular surface point are calculated. Then for each of these neighbor points, its projections on the two images and its corresponding two image brightness values are obtained. Using the inverse of the estimated reflectance function and the two brightness values, the surface orientation of each neighbor point is resolved up to a two-way ambiguity. Based on the 3D locations and surface orientations of these neighbor points and first-order Taylor approximation, the 3D locations are computed over a larger surface area, and using the inverse of the reflectance function and the brightness values of the image correspondences on the larger area, the surface orientations are calculated on the area. In this way, starting from the singular points, the surface depth and orientation can be computed simultaneously over the object surface. The ambiguity can be removed by using integrability constraints [5] or other information, such as image contours and surface points of known 3D locations. The computation for depth basically is an integration process so it is robust against image noise. The computation for surface orientation can be done by look-up table just as in photometric stereo [15, 16].

Section 2 introduces the assumptions and the experimental setting for our work. Section 3 presents a method for building the reflectance function of a rotating object under a collinear light source. Section 4 describes the surface recovery procedure. Section 5 shows some experimental results on real image sequence. The last section discusses experimental results and further work.

2 Assumptions and Experimental Conditions

The imaging geometry is shown in Fig. 1. The object is on a turntable whose rotation angle can be controlled or detected. The Y axis coincides with the rotation axis of the turntable. The light source and the camera are fixed and point in the same direction. The camera viewing direction and

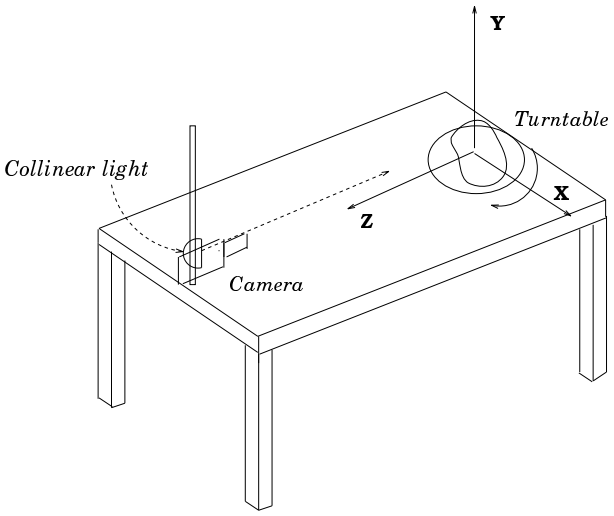

Figure 1: Experimental setup

the light illuminant direction are aligned with the Z axis. The light source is a distant light source with uniform radiance over time and illuminated area. Since the camera is far away from the object, orthographical projection is used. Thus a surface point (x, y, z) is projected on an image point (x, y). To obtain the projection of the rotation axis in the images, a vertical while line on a black board is aligned with the rotation axis and then identified from the image of the board. Images are taken when the object rates around the Y axis in the direction from the X axis to the Z axis.

The surface of the object is piecewise continuous and twice differentiable. The surface orientation is defined as $(p, q, -1)$ with $p = \partial z(x, y)/\partial x$ and $q = \partial z(x, y)/\partial y$. When the object rotates the changes on coordinates and surface orientation can be associated with their original states by a rotational transformation. Let (x, y, z) be a 3D surface point on the object and $(p, q, -1)$ be the surface orientation of this point. After an α degree rotation, the 3D location $(x_\alpha, y_\alpha, z_\alpha)$ of this point is $(x_\alpha,\ y_\alpha,\ z_\alpha) = (x\cos\alpha - z\sin\alpha,\ y,\ x\sin\alpha + z\cos\alpha)$ and the surface orientation $(p_\alpha, q_\alpha, -1)$ of this point is determined by

$$p_\alpha = \frac{p\cos\alpha + \sin\alpha}{\cos\alpha - p\sin\alpha}, \quad (1)$$

$$q_\alpha = \frac{q}{\cos\alpha - p\sin\alpha}. \quad (2)$$

Since each image is taken after the object has rotated by a certain angle, we relate coordinate and surface orientation on the object with the images taken during the rotation. For a surface point, when

we talk about its coordinate or orientation relative to an image we mean the coordinate or orientation of the surface point at the moment that the image is taken.

We also assume the reflectance of the object surface is uniform. In the general case, the image brightness of a 3D point under a distant light source is determined by the reflectance function $R(i, e, g)$ [14]. As shown in Fig. 2, the incident angle i is the angle between the incident ray and the surface normal, the emergent angle e is the angle between the emergent ray and the surface normal, and the phase angle e is the angle between the incident and emergent rays. Under a collinear light source, as shown in Fig. 3, the phase angle g becomes zero and the incident angle i becomes the same as the emergent angle e. In this case, all the components of the reflectance such as the specular component, diffuse component and other components defined in Tagare's paper [11] are functions of the incident angle i only. Under a collinear light source the total image brightness at the surface point becomes a function of one variable, that is, a function of the incident angle i. Thus for the surface point (x, y, z), its image brightness value can be written as

$$E(x, y) = R(i(x, y)) \tag{3}$$

where $i(x, y)$ is the incident angle at point (x, y, z).

The reflectance function has maximum brightness value when $i = 0$ and minimum brightness value when $i = \pi/2$. We assume the function is strictly monotonic. This assumption is true for most surfaces. The most important aspect of the reflectance function $R(i)$ is that it is a function of one variable. This makes the relation between brightness value and surface orientation very simple. The simplicity of the reflectance function makes it easy to estimate the reflectance function and apply the estimated function for surface recovery.

3 Estimating the Reflectance Function

The estimation of the reflectance function is based on some singular points of surface orientation (0, 0, -1) relative to the first image. These singular points also have singular brightness values in the first image because their incident angles are zero. Let the surface point (x_s, y_s, z_s) be one of these points. The values of x_s and y_s can be directly found from the first image by searching for a point of the maximum brightness. To determine z_s, we look at the image taken after the object has rotated by 90 degrees. In

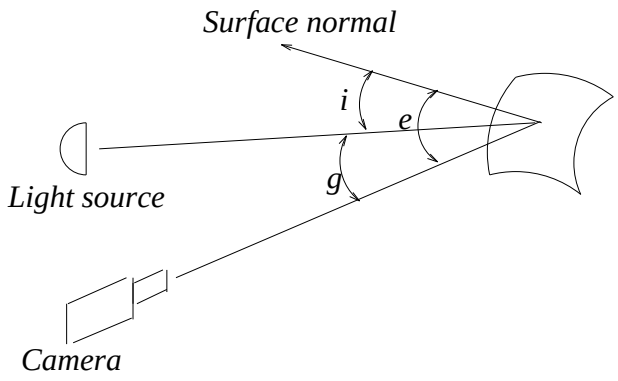

Figure 2: The image brightness is a function of the angles i, e and g.

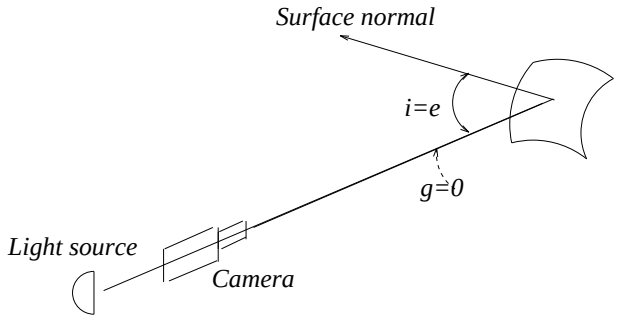

Figure 3: Under a collinear light the image brightness only depends on angle i.

that image, the projection of the singular surface point is $(-z_s, y_s)$. The value for z_s is the horizontal distance from the corresponding contour point to the image of the rotation axis. Finding the corresponding contour point is not difficult since its y coordinate is already known and the tangent line of this point along the contour is parallel to the Y axis. Once we know the 3D locations of these singular points, we can extract the brightness values of these points from the image sequence. For the singular point (x_s, y_s, z_s), after the object has rotated by an angle $\theta_i \leq 90°$, the 3D location of this point $(x_i,\ y_i,\ z_i) = (x_s \cos\theta_i - z_s \sin\theta_i,\ y_s,\ x_s \sin\theta_i + z_s \cos\theta_i)$. The image brightness $E(x_i, y_i)$ of this point can be directly obtained from image point (x_i, y_i) in $image_i$ taken after a θ_i degree rotation of the object. It is easy to show that the incident angle for point (x_i, y_i, z_i) is θ_i. From the brightness $E(x_i, y_i)$ and the corresponding incident angle θ_i, we can build the reflectance function for the surface.

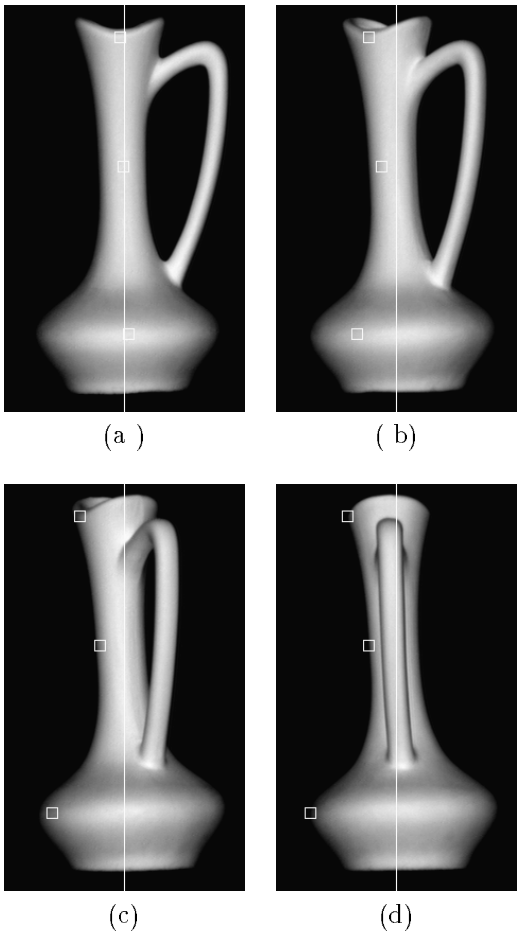

Figure 4: Tracking the singular points over the image sequence

Fig. 5 shows the reflectance function $E = R(i)$ obtained from an image sequence of a rotating vase. The rotation angle between two consecutive images in the image sequence is 5 degree. Thus nineteen images are taken during a 90 degree rotation. The images in Fig. 4 are four images of a rotating vase. The images (a), (b), (c) and (d) are the images taken after 0, 30, 60, and 90 degrees rotation, respectively. Three singular points are extracted from the first image by searching for image points of maximum brightness value and their corresponding contour points in the last image. The white line in the middle of each image is the virtual image of the rotation axis of the object. The centers of the small square boxes in each image denote the three points tracked over the image sequence. The image brightness values are sampled at every 5° in the range from 0° to 90° of the incident angle. The average of the brightness values of the three points is used to build

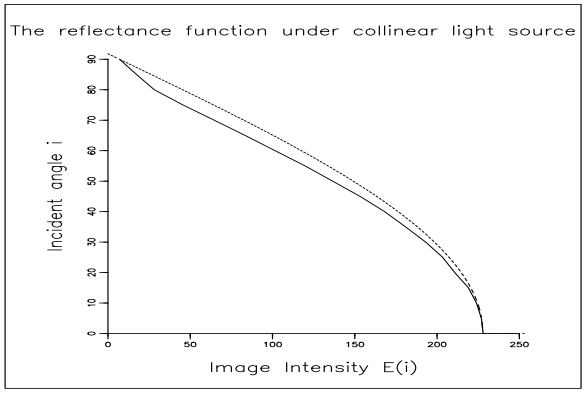

Figure 5: The reflectance function obtained from the image sequence

the reflectance function. Since the reflectance function is strictly monotonic, its inverse exists. The function we actually used for surface recovery is the inverse function $i = R^{-1}(E)$. The inverse function is linearly interpolated for every integer brightness value ranging from 0 to 255.

4 Surface Recovery

After the reflectance function has been obtained, surface recovery can be done by using any two images in the image sequence of a rotating object. In this paper, the first image and the image taken after the object has rotated by a certain angle are used. The depth and surface orientation are computed at every point in the first image. Surface recovery uses two subprocedures to compute the depth and surface orientation. The first subprocedure does local expansion of depth by using first-order Taylor series approximation. For an image point (x, y), if the depth z and the surface orientation $(p, q, -1)$ are known, the depth z' of an image point $(x+\delta x, y+\delta x)$ in the small neighborhood of the image point (x, y) is calculated by $z' = z + \delta z = z + p\delta x + q\delta y$. The second subprocedure determines surface orientation (up to a two-way ambiguity) from image brightness values of a surface point in the two images. The following calculation shows how we derive orientation from image brightness.

Let $image_0$ be the image taken before the rotation of the object and $image_1$ be the image taken after an α degree rotation of the object. Let (x_0, y_0) and (x_1, y_1) be the projections of a 3D surface point in $image_0$ and $image_1$ respectively and their brightness values are $E(x_0, y_0)$ and $E(x_1, y_1)$. Using the inverse reflectance function $i = R^{-1}(E)$, we obtain the incident angle i_0 and i_1 from $E(x_0, y_0)$

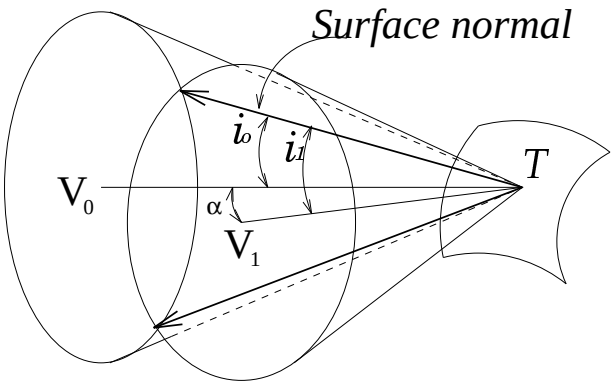

Figure 6: The solution for surface orientation

and $E(x_1, y_1)$. Let the surface orientation of the 3D point be $(p_0, q_0, -1)$ relative to $image_0$ and and the surface orientation of the same 3D point be $(p_1, q_1, -1)$ relative to with $image_1$. From the definition of incident angle and the transformation between the object coordinates, we have

$$\cos i_0 = \frac{1}{\sqrt{p_0^2 + q_0^2 + 1}}, \tag{4}$$

$$\cos i_1 = \frac{1}{\sqrt{p_1^2 + q_1^2 + 1}}, \tag{5}$$

$$p_1 = \frac{p_0 \cos\alpha + \sin\alpha}{\cos\alpha - p_0 \sin\alpha}, \tag{6}$$

and

$$q_1 = \frac{q_0}{\cos\alpha - p_0 \sin\alpha}. \tag{7}$$

Substituting p_1 and q_1 in Equation 5, we get

$$\cos i_1 = \frac{1}{\sqrt{1 + (\frac{p_0\cos\alpha + \sin\alpha}{\cos\alpha - p_0\sin\alpha})^2 + (\frac{q_0}{\cos\alpha - p_0\sin\alpha})^2}}; \tag{8}$$

The equation can be simplified to

$$\cos i_1 = \cos i_0(\cos\alpha - p_0 \sin\alpha). \tag{9}$$

Solving Equation 9 for p_0 and from Equation 4, we have

$$p_0 = \frac{1}{\tan\alpha} - \frac{\cos i_1}{\cos i_0 \sin\alpha}, \tag{10}$$

$$q_0 = \pm\sqrt{\frac{1}{\cos i_0^2} - p_0^2 - 1}. \tag{11}$$

The geometric explanation for the solution of p_0 and q_0 is shown in Fig. 6. Here we assume $image_0$ and $image_1$ are taken from two different viewing directions with the object fixed. We denote the viewing direction for $image_0$ as vector v_0 and the viewing direction for $image_1$ as vector v_1. All the surface normals with incident angle i_0 to the viewing direction vector v_0 form a cone. All the surface normals with incident angle i_1 to the viewing direction v_1 form another cone. The intersection of the two cones is two vectors. The two vectors are symmetric about the XZ plane. Only one of the two vectors overlaps with the surface normal. So there is a two-way ambiguity in the solution for surface orientation which is caused by the two solutions for q_0 in Equation 11.

The surface recovery procedure starts at the image points whose depth and surface orientations are known. These starting points could be the singular points we used to estimate the reflectance function. For each starting point of known depth, we use the first subprocedure to compute the depth for the neighbors of the starting point. For each neighbor point, using the depth value computed by the first subprocedure, we compute its projections on the two images and extract the two brightness values from the two images. Then we use the second subprocedure with the two brightness values extracted to compute surface orientation for every neighbor point. Using the first subprocedure on the neighbor points, we expand the depth over a larger area. Using the second subprocedure on the larger area, we compute surface orientation for the larger area. By iteratively applying the first and the second subprocedures, we spread the computation over the whole image to obtain the depth and surface orientation at the same time. The number of local operations in this process is linear in the number of pixels in the image.

5 Experimental Results

In our experiment, we use a calibrated image facility (CIF) [16] built in our lab to control the rotation of the object and the imaging condition. Although the camera we used is a 24-bit RGB camera, we only use one of the three B&W images. We use a DC powered beamed light source and mount it on the top of the camera. The light source and the camera point in the same direction to the object on a turntable. We considered putting a half-silvered mirror in front of the camera to make the viewing direction and illuminant direction precisely collinear, but it turned out to be unnecessary because we did not observe the effects caused by the small angle between the viewing direction and the illuminant direction. In practice, the radiance of the light source

is not constant over illuminated area. We use a uniform white board to calibrate the non-uniform illumination. Since the distance from the camera to the object is far bigger than the size of the object, the camera is set to telephoto mode and orthographical projection is used for a reasonable approximation. The actions of rotating an object and taking images of the object are well synchronized by a computer. Nineteen images of a vase are taken with a 5° interval between two adjacent images. Thus the total rotation of the vase is 90 degrees.

To filter image noise and quantization noise, the images are smoothed with a Gaussian filter of $\sigma = 1$. Four images from the image sequence of the vase are shown in Fig. 4. Images (a), (b), (c) and (d) are, respectively, the images taken after 0, 30, 60 and 90 degrees rotation of the vase. The estimated reflectance function of the vase is shown in Fig. 5. We track the three singular points starting from the first image to estimate the reflectance function. The brightness value for the reflectance function is the average of the brightness values of the three points. The singular surface points relative to the last image can also be used for better estimation. For the time being, only the singular points relative to the first image are used.

In surface recovery the first image (Fig. 7(a)) and the image after a 5 degree rotation (Fig. 7(b)) are used. We first compute depth and surface orientation along a line in the y direction starting from the singular point in the lower body part of the vase. Later on the 3D points on this line are used as starting points for computation along the x direction. In Fig 7(a)), the center of the small box denotes the starting point for surface recovery and the white line is the line along which depth and surface orientation are first computed. Fig. 7(c) shows the depth along this line. The horizontal distance from a point on the curve to the middle black straight line is the depth. Depth and orientation are expressed in the coordinate system related to the first image. During surface recovery, depth and orientation are computed at every pixel in the first image. The image brightness value of a 3D point in the second image are interpolated between pixels as the projection of a 3D point may be located between pixels in the second image. The surface plot of the recovered vase are shown in Fig. 8. The surface plot is displayed with Matlab by using the depth data calculated over the first image. We did not do any smoothing or regularization on the depth and surface orientation data.

When we compute a new depth value z' in the y direction, we have $z' = z + q\delta y$. Thus the am-

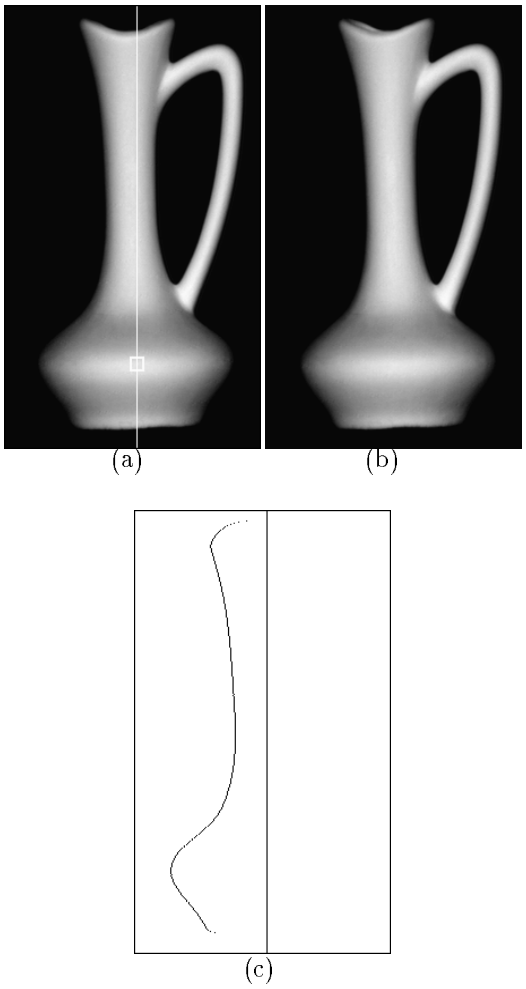

Figure 7: Images used for surface recovery and the depth along the vertical line in (a)

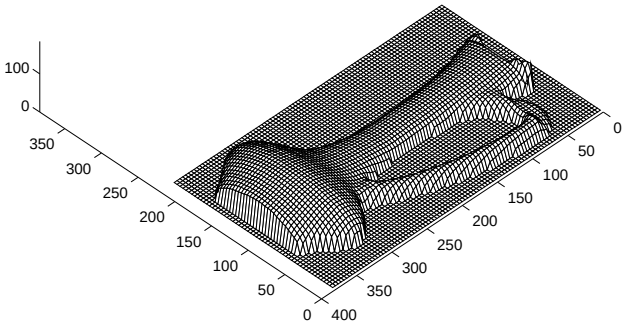

Figure 8: The height plot of the recovered surface

biguity in depth occurs as there are two solutions of q obtained from Equation 11. During the surface recovery procedure the surface is constructed by using the two possible values of q. Two different surfaces are constructed at the beginning. The two partially constructed surfaces are projected back on the last image in the image sequence. The contours in the last image are checked against the contours in the images of the two partially constructed surfaces. The partial surface whose contours are not consistent with those in the last image is discarded. The other partial surface is used to recover the remaining part of the surface with the continuous constraint. This ambiguity can also be removed by the integrability constraint [5]. For the two partially constructed surfaces, s_0 and s_1, with two continuous values q_0 and q_1, we compare $\int_{s_0}(\frac{\partial q_0}{\partial x} - \frac{\partial p}{\partial y})^2$ with $\int_{s_1}(\frac{\partial q_1}{\partial x} - \frac{\partial p}{\partial y})^2$ and abandon the surface with the bigger integral.

6 Discussion and Further Work

The results obtained shows that the technique is feasible and robust for surface recovery. We don't assume the reflectance function has any particular form. We estimate the reflectance function directly from the image sequence of a rotating object. The surface recovery procedure exploits the photometric constraint through the reflectance function and the geometric constraint by using first-order Taylor series approximation and rotational transformation. The subprocedure for calculating surface depth integrates surface orientation. So in theory this procedure is robust against image noise. The perturbation on depth value of the starting point only affect the surface depth near the starting point and do not change the surface depth which is far from the starting point. Shifting the rotation axis 3 or 4 pixels does not make much difference on the final results.

We have not made a detailed error analysis on the surface recovery process. From the surface plot in Fig. 8 we can observe some errors. These errors mainly come from three sources: inaccurate estimation of the reflectance function, non-uniform albedo over the object surface and interreflection on the object. To reduce the error in the estimation of the reflectance function, we can use more singular points or use other surface points whose surface orientation and 3D location can be computed by image cues such as contours [17]. To reduce the error caused by non-uniform albedo, we can extract the reflectance function for a local area of relatively constant albedo and use the local reflectance function for the local surface recovery. This idea can be applied to surfaces of piecewise uniform reflectance. This is our current area of research. Reducing the error caused by interreflection in the general case is very hard [3]. So far we do not have effective methods for removing interreflection on surfaces with non-Lambertian reflectance.

Beside shading, there are other kinds of cues such as contour and stereo available from image sequence of a rotating object. These cues can be used in different ways. One way to use the contour is to get local reflectance function from contours. In our work we use singular points to estimate the reflectance function and assume these points will be visible during the 90° rotation. It has been shown that contours in an image sequence of a rotating object can be used to compute the location and orientation of some surface points [17]. These surface points can be alternatives for singular points. One way to use the stereo information is to get the 3D locations of some surface points from surface features and use these points as starting points for our surface recovery procedure. The stereo information can also be used to remove the ambiguity on the q component of surface orientation. The integration of all the cues is not an easy task [9, 10, 7, 18, 1]. extending our work to surfaces with piecewise uniform reflectance will require integrating different cues.

Another extension of our work is surface recovery by rotating the object more than 90 degrees. In this way, we can get more singular points and obtain a more accurate estimate of the surface reflectance function. Also we can construct the whole object by integrating surface depth recovered from different views. We intend to apply our surface recovery method and its extensions in automatic modeling, fast prototyping, surface inspection for Computer Graphics, CAD and CAM.

7 Acknowledgments

We would like to thank Yuji Iwahori, Esfandiar Bandari and Jeffery Beis for their useful comments. The author's email address are jplu@cs.ubc.ca and little@cs.ubc.ca. This research was supported by grants from the Natural Sciences and Engineering Research Council of Canada and the Networks of Centres of Excellence Institute for Robotics and Intelligent Systems, Projects A-1 and ISDE-6.

References

[1] P. Fua and Y.G. Leclerc. Using 3-dimensional meshes to combine image-based and geometry-based constraints. In *Proc. 3rd European Conference on Computer Vision*, pages 282–291, May 1994.

[2] B. K. P. Horn and M. J. Brooks, editors. *Shape from Shading*. MIT Press, Cambridge, MA, 1989.

[3] S. K. Nayar, K. Ikeuchi, and T. Kanade. Shape from interreflections. *International Journal of Computer Vision*, 6(3):173–195, 1991.

[4] Shree K. Nayar, Katsushi Ikeuchi, and Takeo Kanade. Determining shape and reflectance of hybrid surfaces by photometric sampling. *IEEE Transactions on Robotics and Automation*, 6(4):418–431, 1990.

[5] Ruth Onn and Alfred Bruckstein. Integrability disambiguates surface recovery in two-image photometric stereo. *International Journal of Computer Vision*, 5(1):105–113, 1990.

[6] Michael Oren and Shree K. Nayar. Seeing beyond Lambert's law. In *Proc. 3rd European Conference on Computer Vision*, pages 269–280, May 1994.

[7] Sharath Pankanti, Anil K. Jain, and M. Tuceryan. On integration of vision modules. In *Proc. IEEE Conf. Computer Vision and Pattern Recognition, 1994*, pages 316–322, June 1994.

[8] A. P. Pentland. Local shading analysis. *IEEE Transactions on Pattern Analysis and Machine Intelligence*, 6:170–187, 1984.

[9] T. Poggio, E. Gamble Jr., and J. J. Little. Parallel integration of vision modules. *Science*, 242(4877):436–440, October 1988.

[10] R. Szeliski. Shape from rotation. In *Proc. IEEE Conf. Computer Vision and Pattern Recognition, 1991*, pages 625–630, June 1991.

[11] Hemant D. Tagare and Rui J.P. deFigueiredo. A theory of photometric stereo for a class of diffuse non-Lambertian surfaces. *IEEE Transactions on Pattern Analysis and Machine Intelligence*, 13(2):133–152, 1991.

[12] Lawrence B. Wolff. Shape understanding from Lambertian photometric flow fields. In *Proc. IEEE Conf. Computer Vision and Pattern Recognition, 1989*, pages 46–52, June 1989.

[13] Lawrence B. Wolff. Diffuse reflection. In *Proc. IEEE Conf. Computer Vision and Pattern Recognition, 1992*, pages 472–478, June 1992.

[14] R. J. Woodham. Photometric method for determining surface orientation from multiple images. *Optical Engineering*, 19:139–144, 1980.

[15] R. J. Woodham. Determining surface curvature with photometric stereo. In *IEEE Conf. Robotics & Automation*, pages 36–42, Scottsdale, AZ, 1989.

[16] R. J. Woodham. Gradient and curvature from photometric stereo including local confidence estimation. *Journal of the Optical Society of America*, 11(11):3050–3068, November 1994.

[17] J. Y. Zheng. Acquiring 3-D models from sequences of contours. *IEEE Transactions on Pattern Analysis and Machine Intelligence*, 16(2):163–178, 1994.

[18] J. Y. Zheng and Fumio Kishino. Verifying and combining different visual cues into a 3D model. In *Proc. IEEE Conf. Computer Vision and Pattern Recognition, 1992*, pages 777–780, June 1992.